

To appear in Astrophysical Journal Letters

An Interaction of a Magellanic Leading Arm High Velocity Cloud with the Milky Way Disk

N. M. McClure-Griffiths,¹ L. Staveley-Smith,² Felix J. Lockman,³ M. R. Calabretta,¹ H. Alyson Ford,^{1,4} P. M. W. Kalberla,⁵ T. Murphy,^{6,7} H. Nakanishi,^{1,8} D. J. Pisano³

ABSTRACT

The Leading Arm of the Magellanic System is a tidally formed H I feature extending $\sim 60^\circ$ from the Magellanic Clouds ahead of their direction of motion. Using atomic hydrogen (H I) data from the Galactic All Sky-Survey (GASS), supplemented with data from the Australia Telescope Compact Array, we have found evidence for an interaction between a cloud in the Leading Arm and the Galactic disk where the Leading Arm crosses the Galactic plane. The interaction occurs at velocities permitted by Galactic rotation, which allows us to derive a kinematic distance to the cloud of 21 kpc, suggesting that the Leading Arm crosses the Galactic Plane at a Galactic radius of $R \approx 17$ kpc.

Subject headings: galaxies: interactions — Galaxy: structure — Magellanic Clouds

¹Australia Telescope National Facility, CSIRO, Marsfield NSW 2122, Australia; naomi.mcclure-griffiths@csiro.au, mark.calabretta@csiro.au

²School of Physics, University of Western Australia, Crawley WA 6009, Australia; lister.staveley-smith@uwa.edu.au

³National Radio Astronomy Observatory, Green Bank, WV 24944; jlockman@nrao.edu, dpisano@nrao.edu

⁴Centre for Astrophysics and Supercomputing, Swinburne University of Technology, Hawthorn VIC 3122, Australia; alyson@astro.swin.edu.au

⁵Argelander-Institut für Astronomie, Universität Bonn, 53121 Bonn, Germany; pkalberla@astro.uni-bonn.de

⁶School of Physics, University of Sydney, NSW 2006, Australia; tara@physics.usyd.edu.au

⁷School of Information Technologies, University of Sydney, NSW 2006, Australia

⁸Present address: Faculty of Science, Kagoshima University, Kagoshima 890-0068, Japan; hnakanis@sci.kagoshima-u.ac.jp

1. Introduction

The Magellanic System is engaged in a complicated interaction with the Milky Way, which has created a trailing “Magellanic Stream” (Wannier & Wrixon 1972), and a tidal “Leading Arm” of H I. The Leading Arm has a metallicity similar to that of the Magellanic Clouds and a consistent velocity structure from its origin in the Clouds at $b \lesssim -25^\circ$, through the Galactic equator, to $b \approx +30^\circ$ (Mathewson et al. 1974; Putman et al. 1998; Lu et al. 1998; Brüns et al. 2005). Model orbits for the Magellanic Clouds (Yoshizawa & Noguchi 2003; Connors et al. 2006) have predicted that the Leading Arm should cross the Milky Way disk some 30 - 60 kpc from the Sun, but there are no observational constraints on this distance. New proper motion measurements suggest that the Magellanic Clouds may be moving faster than previously thought, implying a larger crossing distance for the Leading Arm than earlier models (Kallivayalil et al. 2006b,a).

High velocity cloud HVC 306-2+230, centered at $(l, b, v) = (305.7^\circ, -0.8^\circ, 220 \text{ km s}^{-1})$, is one of the many clouds that make up the Magellanic Leading Arm (Mathewson et al. 1979; Brüns et al. 2005) and is of particular interest because it is one of two that cross the Galactic equator. Brüns et al. (2005) suggested that this HVC shows evidence of a ram-pressure interaction with the Galactic disk. Using new H I data from the Galactic All-Sky Survey (McClure-Griffiths et al. 2006; McClure-Griffiths et al. 2007, in prep), together with high resolution H I data from the Australia Telescope Compact Array (ATCA), we present evidence of interaction between HVC 306-2+230 and the disk of the Milky Way (§3). We use the interaction to derive a kinematic distance to the Leading Arm where it crosses the Galactic Plane (§3.1). Finally, in §4 we discuss the implications the distance places on the orbit of the Magellanic Clouds.

2. Data

The H I data discussed here were obtained as part of the Galactic All-Sky Survey (GASS; McClure-Griffiths et al. 2006; McClure-Griffiths et al. 2007, in prep), which used the 21cm multibeam receiver on the Parkes Radio Telescope to map Galactic and Magellanic H I emission over the entire sky south of Declination $\delta = 0^\circ$. The project will be described in full detail in a separate paper. For the purposes of the current paper, the techniques for data-taking and analysis are the same as in McClure-Griffiths et al. (2006). Since the 2006 paper, the full dataset has been obtained and is used for this analysis, with an angular resolution of $15'$, channel spacing of 0.8 km s^{-1} , and an rms brightness temperature $1-\sigma$ noise of $\sim 60 \text{ mK}$.

We also make use of high resolution H I data from the Australia Telescope Compact Array (ATCA). We have combined archival data from the Southern Galactic Plane Survey (SGPS; McClure-Griffiths et al. 2005) together with a new 10 hr ATCA observation with the hybrid array configuration, H168. The SGPS data consist of observations obtained with the 375, 750A, B, C, and D array configurations of the ATCA. The multi-pointing ATCA data were jointly imaged using natural weighting, deconvolved, and restored with a synthesised beam of $100''$, and combined with the low resolution data from GASS for sensitivity to angular scales from $100''$ to several degrees. The ATCA data are limited to Galactic latitudes $|b| < 1.0^\circ$ and have an rms brightness temperature $1-\sigma$ noise of ~ 1.3 K.

3. Evidence of a High Velocity Cloud Impact with the Galactic Disk

We have used H I data from GASS to search for any indication of interaction between HVC 306-2+230 and the Milky Way disk. Figure 1 shows Galactic H I emission at $v_{LSR} = 91$ km s $^{-1}$ and $v_{LSR} = 122$ km s $^{-1}$, overlaid with the column density contours of HVC 306-2+230. There is a morphological match between the Galactic H I emission and the HVC. At $v_{LSR} = 91$ km s $^{-1}$ the Galactic H I traces the bottom and sides of the HVC, while at $v_{LSR} = 122$ km s $^{-1}$ a ridge of Galactic H I wraps around the head of the cloud. The high resolution data show that the ridge is very thin, only $3 - 5$ arcminutes, and seems to be cold. Spectra taken through the ridge ($b = 1.2^\circ$), the head of the HVC ($b = 0.5^\circ$) and its tail ($b = -0.2^\circ$) are shown in Figure 2. All show a strong, broad feature at $v \approx 100$ km s $^{-1}$, but towards the ridge there is an additional narrow feature at $v = 122$ km s $^{-1}$. The H I linewidth in the ridge is $\Delta v \sim 4$ km s $^{-1}$ (FWHM), implying a temperature of $T \leq 350$ K. There is evidence for the development of the 122 km s $^{-1}$ feature near the head of the HVC at a latitude of $b = 0.5^\circ$.

The context of the interaction is shown in Figure 3, in a longitude-velocity cut through the data at $b = 0.37^\circ$, near the tip of the cloud. The H I around 120 km s $^{-1}$, which forms the ridge in Figure 1(b), is seen to be confined to longitudes between HVC 306-2+230 and a second Leading Arm cloud at $l = 312^\circ$. The data thus suggest that the HVCs are interacting with gas originally at $v_{LSR} \approx 90$ km s $^{-1}$ to produce the ridge near $v_{LSR} = 122$ km s $^{-1}$ around the head of the HVC.

HVC 306-2+230 itself shows evidence of interaction. The high-resolution ATCA data of Figure 4 show that it has a very bright, $T_b = 15 - 20$ K, narrow bow-shaped ridge of emission along the head of the cloud with dense clumps along the bent tail. The column density along the bright ridge is $N_{HI} \sim 10^{20}$ cm $^{-2}$. Spectra toward the head of the cloud have a two velocity-component structure; one very narrow component of FWHM $\Delta v = 4.9$

km s⁻¹ and a second, broader component of width $\Delta v = 16.9$ km s⁻¹. This is consistent with a two-phase structure of the cloud, where one component has $T \leq 600$ K and the other $T \leq 6000$ K. The velocity width of the spectra increases with distance along the tail; spectra at $b = -1.6^\circ$ and $b = -2.4^\circ$ have FWHM of $\Delta v = 21.6$, and 27.8 km s⁻¹, respectively.

The structure of the disk emission and the HVC resemble simulations of HVCs impacting the Galactic disk which predict that a moderately dense HVC travelling at ~ 100 km s⁻¹ with respect to the disk, will form a hemispherical shell of cool, dense H I ahead of it (Tenorio-Tagle et al. 1987; Comeron & Torra 1992). The newly formed shell will be accelerated by the interaction. High resolution simulations of HVCs moving through uniform media show that a very thin, bow-shaped structure develops along the leading edge of the cloud (Quilis & Moore 2001; Konz et al. 2002; Agertz et al. 2007), much like the high resolution structure of the HVC shown in Figure 4. HVC disk impact simulations also predict that there should be a layer of hot, ionized gas between the neutral HVC and the neutral disk. Although ionized gas around HVC 306-2+230 would not be detectable in H α or soft X-ray emission because of absorption by foreground gas in the Galactic plane, there is a significant offset between the head of the HVC and the Galactic H I at $v_{LSR} = 122$ km s⁻¹, which is consistent with the presence of a layer of ionized gas. The separation between the HVC head and H I ridge in the high resolution ATCA data is $\sim 0.6^\circ$, or ~ 200 pc at $d = 21$ kpc. The agreement between the observations and simulations of HVC cloud impacts is additional evidence that HVC 306-2+230 is interacting with the Milky Way disk.

3.1. Distance to the HVC

The data presented here suggest that the HVC interacts with gas initially at $v_{LSR} \approx 90$ km s⁻¹, which implies that the interaction takes place well into the outer Galaxy. We can use the velocity of the interaction region to estimate a kinematic distance to the HVC. Because the HVCs are at a more positive velocity than disk gas, any transfer of momentum from the HVC to the disk will result in a more positive velocity for the disk gas, erroneously increasing the kinematic distance. Our distance estimates are thus upper limits. Assuming a flat rotation curve, where $\Theta(R) = \Theta_0 = 220$ km s⁻¹ and a Sun-Galactic Center distance of $R_0 = 8.5$ kpc, we estimate that the emission is at a Galactocentric radius of $R \approx 17$ kpc and a heliocentric distance of $d \approx 21$ kpc. Use of a different rotation curve or Sun-center distance (e.g., 8.0 kpc) changes these values by no more than 20%.

That we observe neutral gas with which the HVC is interacting also provides an upper limit to the distance by placing it within the detectable H I disk of the Galaxy. Although the exact extent of the Galactic H I disk is uncertain, estimates are that by 50 kpc radius

the H I surface density is less than $10^{-2} \text{ M}_\odot \text{ pc}^{-2}$ (Knapp et al. 1978) and the majority of the H I is within 30 kpc (Nakanishi & Sofue 2003; Levine et al. 2006). The ridge of H I at 120 km s^{-1} , if interpreted as material swept-up by the HVC, can give some information on the environment the HVC is encountering. The ridge has $N_{\text{HI}} = 7 - 10 \times 10^{19} \text{ cm}^{-2}$ so if its line-of-sight extent is similar to its transverse extent ($\approx 60'$) then the column density in the z -direction ($< 15'$, perpendicular to the motion of the HVC) is independent of distance and simply the observed N_{HI} scaled by the ratio of widths, $15/60$. Given the maximum vertical extent of the ridge, the column density perpendicular to the line of sight is $N_H < 2 - 4 \times 10^{19} \text{ cm}^{-2}$, equivalent to $1 - 3 \times 10^{-1} \text{ M}_\odot \text{ pc}^{-2}$. This is an incomplete accounting of the disk gas the HVC would encounter, neglecting inhomogeneities in the medium and the mass of ionized and molecular material, but nonetheless indicates that the upper limit on the HVC distance is $R < 30 \text{ kpc}$.

3.2. HVC Drag Interaction

Figure 5 is a latitude-velocity slice taken at $l = 305.6^\circ$ through the center of HVC 306-2+230. The cloud shows a velocity gradient of about -30 km s^{-1} between $b = -4.4^\circ$, where the central velocity is $v_{\text{LSR}} \approx 252 \text{ km s}^{-1}$, and $b = -1.5^\circ$, where $v_{\text{LSR}} \approx 223 \text{ km s}^{-1}$. The gradient is large and in the wrong sense to arise from either the projection effects of the Sun’s motion or the upward (toward positive latitudes) motion of the HVC as implied by its head-tail morphology and the expected trajectory of the Leading Arm. The gradient must be intrinsic to the HVC, and may arise from a deceleration as the HVC goes through the disk of the Milky Way. Benjamin & Danly (1997) showed that drag forces should slow a cloud as it nears the Galactic plane. We cannot measure the z velocity of the HVC, but we can estimate the change in velocity with height if the cloud were falling at the terminal velocity; given in equation 2 of Benjamin & Danly (1997). For a cloud of column density $\sim 2 \times 10^{19} \text{ cm}^{-2}$, approaching a Gaussian disk with a midplane density $n = 0.04 \text{ cm}^{-3}$ and a scale height of 1 kpc, the difference in terminal velocity between $z = 1400 \text{ pc}$ and $z = 200 \text{ pc}$ is $\sim 30 \text{ km s}^{-1}$, which matches the observed velocity variation along the length of the cloud. This adds further support to the evidence that the HVC is interacting with the Galactic disk; at very large Galactic radii there would be insufficient gas to cause significant drag.

4. Discussion of the Magellanic Orbits

Many simulations of the Magellanic System have attributed the origin of the Leading Arm to a close pass between the SMC and the Milky Way which stripped gas from

the SMC that was eventually pulled into a leading tidal feature (e.g. Connors et al. 2006; Yoshizawa & Noguchi 2003). Alternative theories give the Leading Arm an LMC origin (e.g. Mastropietro et al. 2005). All of these simulations, however, rely on a past close encounter between the Magellanic Clouds and the Milky Way. From this encounter the Connors et al. (2006) and Yoshizawa & Noguchi (2003) simulations have predicted that the Leading Arm crosses the Galactic plane at a distance of $30 - 60$ kpc from the Sun. Our newly derived distance of 21 kpc is smaller than the lower limit of these predictions.

These models do not take into account recently revised measurements of the proper motions of the LMC and SMC, which have shown that the Magellanic Clouds have much higher tangential velocities than previous thought (van der Marel et al. 2002; Kallivayalil et al. 2006b). Re-calculation of the LMC orbit based on these proper motions and new mass models for the Milky Way suggest that the LMC may be on its first pass and currently at perigalacticon (Besla et al. 2007). If true, and the SMC has a similar orbit, this would have profound implications on the formation models for the Leading Arm. Rather than relying on close past interactions with the Milky Way to strip LMC/SMC gas, these orbits would require an alternative method of extracting gas from the galaxies, such as the blowout model suggested by Nidever et al. (2007).

Besla et al. (2007) do not predict the future orbit of the LMC, but we can make a very simple estimate of where the LMC will cross the Galactic plane by extrapolating from the current position, assuming a constant LMC space velocity and neglecting Milky Way gravity. In a Cartesian system centred on the Galactic center where the LMC is at $(x_0, y_0, z_0) = (-1, -41, -27)$ kpc, with a velocity vector $(v_x, v_y, v_z) = (-86, -268, +252)$ km s $^{-1}$ (Kallivayalil et al. 2006b), assuming that the time to reach the Galactic plane is $t = -z_0/v_z$, its position at t will be $(-10, -70, 0)$ kpc or $R \sim 71$ kpc. Because we have excluded the gravitational effect of the Milky Way this estimate will be an upper limit. Finally, it has been shown that tidal features can deviate significantly from the orbits of their parent satellites (Connors et al. 2006; Choi et al. 2007), which may also help reconcile the new proper motions with our Leading Arm crossing distance.

5. Summary

We have found evidence for an interaction between one of the Leading Arm High Velocity Clouds, HVC 306-2+230, and the Milky Way disk. As the Leading Arm crosses the Galactic equator it produces a ridge of H I at a velocity of $v_{LSR} = 122$ km s $^{-1}$. Further evidence for the interaction is given by the head-tail structure of the HVC itself, its varying velocity width, the deceleration of the cloud head, and the agreement between simulations of HVC impacts

and the morphology of the HVC and the disk gas. As a rare example of an HVC caught interacting with the disk, HVC 306-2+230 offers a unique opportunity to compare in detail observations with simulations of HVC impacts; this will be the topic of a future paper. The interaction with H I at Galactic velocities has allowed us to estimate a kinematic distance to the Leading Arm of $d \approx 21$ kpc from the Sun or a Galactocentric radius of $R \approx 17$ kpc, with an upper limit of $R < 30$ kpc. This distance is close to that predicted by the Connors et al. (2006) and Yoshizawa & Noguchi (2003) models of the Magellanic system, and smaller than might be expected from the Kallivayalil et al. (2006b) LMC proper motion measurements. Our new Leading Arm distance will provide an important constraint to future models of the Magellanic System as they take into account revised LMC and SMC proper motions.

The Parkes Radio Telescope and the Australia Telescope Compact Array are part of the Australia Telescope which is funded by the Commonwealth of Australia for operation as a National Facility managed by CSIRO. We are grateful to P. Edwards for the allocation of Director's Time at the ATCA to image this HVC and to an anonymous referee for helpful comments.

REFERENCES

Agertz, O., Moore, B., Stadel, J., Potter, D., Miniati, F., Read, J., Mayer, L., Gawryszczak, A., Kravtsov, A., Nordlund, Å., Pearce, F., Quilis, V., Rudd, D., Springel, V., Stone, J., Tasker, E., Teyssier, R., Wadsley, J., & Walder, R. 2007, MNRAS, 380, 963

Benjamin, R. A. & Danly, L. 1997, ApJ, 481, 764

Besla, G., Kallivayalil, N., Hernquist, L., Robertson, B., Cox, T. J., van der Marel, R. P., & Alcock, C. 2007, ApJ, 668, 949

Brüns, C., Kerp, J., Staveley-Smith, L., Mebold, U., Putman, M. E., Haynes, R. F., Kalberla, P. M. W., Muller, E., & Filipovic, M. D. 2005, A&A, 432, 45

Choi, J.-H., Weinberg, M. D., & Katz, N. 2007, MNRAS, 381, 987

Comeron, F. & Torra, J. 1992, A&A, 261, 94

Connors, T. W., Kawata, D., & Gibson, B. K. 2006, MNRAS, 371, 108

Kallivayalil, N., van der Marel, R. P., & Alcock, C. 2006a, ApJ, 652, 1213

Kallivayalil, N., van der Marel, R. P., Alcock, C., Axelrod, T., Cook, K. H., Drake, A. J., & Geha, M. 2006b, *ApJ*, 638, 772

Knapp, G. R., Tremaine, S. D., & Gunn, J. E. 1978, *AJ*, 83, 1585

Konz, C., Brüns, C., & Birk, G. T. 2002, *A&A*, 391, 713

Levine, E. S., Blitz, L., & Heiles, C. 2006, *Science*, 312, 1773

Lu, L., Sargent, W. L. W., Savage, B. D., Wakker, B. P., Sembach, K. R., & Oosterloo, T. A. 1998, *AJ*, 115, 162

Mastropietro, C., Moore, B., Mayer, L., Wadsley, J., & Stadel, J. 2005, *MNRAS*, 363, 509

Mathewson, D. S., Cleary, M. N., & Murray, J. D. 1974, *ApJ*, 190, 291

Mathewson, D. S., Ford, V. L., Schwarz, M. P., & Murray, J. D. 1979, in *IAU Symposium*, Vol. 84, The Large-Scale Characteristics of the Galaxy, ed. W. B. Burton, 547–556

McClure-Griffiths, N. M., Dickey, J. M., Gaensler, B. M., Green, A. J., Havercorn, M., & Strasser, S. 2005, *ApJS*, 158, 178

McClure-Griffiths, N. M., Ford, A., Pisano, D. J., Gibson, B. K., Staveley-Smith, L., Calabretta, M. R., Kalberla, P. M. W., & Dedes, L. 2006, *ApJ*, 638, 196

Nakanishi, H. & Sofue, Y. 2003, *PASJ*, 55, 191

Nidever, D. L., Majewski, S. R., & Butler Burton, W. 2007, *ArXiv e-prints*, 706

Putman, M. E., Gibson, B. K., Staveley-Smith, L., Banks, G., Barnes, D. G., Bhatal, R., Disney, M. J., Ekers, R. D., Freeman, K. C., Haynes, R. F., Henning, P., Jerjen, H., Kilborn, V., Koribalski, B., Knezeck, P., Malin, D. F., Mould, J. R., Oosterloo, T., Price, R. M., Ryder, S. D., Sadler, E. M., Stewart, I., Stootman, F., Vaile, R. A., Webster, R. L., & Wright, A. E. 1998, *Nature*, 394, 752

Quilis, V. & Moore, B. 2001, *ApJ*, 555, L95

Tenorio-Tagle, G., Franco, J., Bodenheimer, P., & Rozyczka, M. 1987, *A&A*, 179, 219

van der Marel, R. P., Alves, D. R., Hardy, E., & Suntzeff, N. B. 2002, *AJ*, 124, 2639

Wannier, P. & Wrixon, G. T. 1972, *ApJ*, 173, L119

Yoshizawa, A. M. & Noguchi, M. 2003, *MNRAS*, 339, 1135

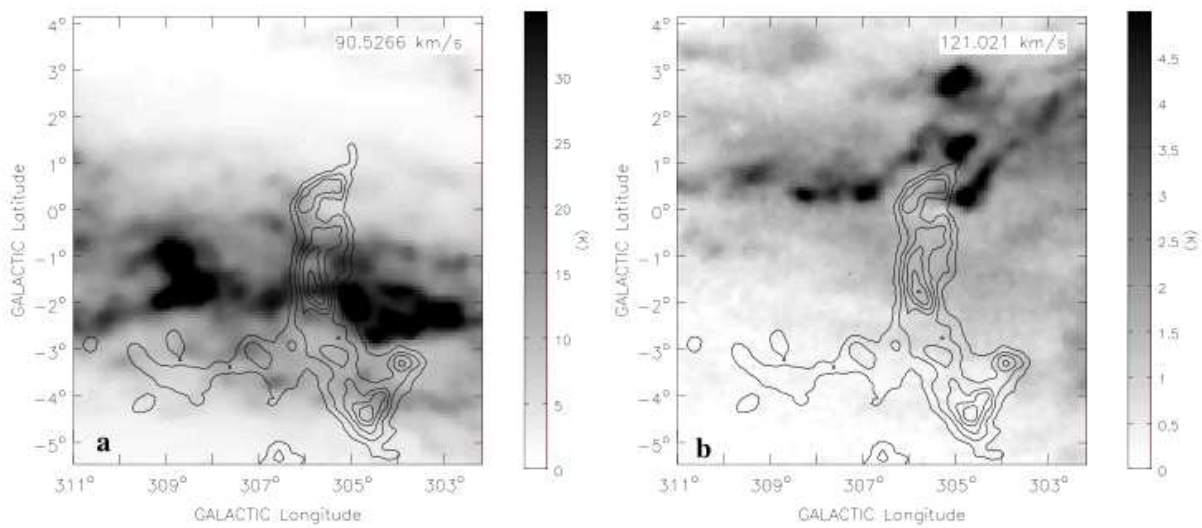


Fig. 1.— H I emission from the Galactic disk (greyscale) overlaid with column density, N_H , contours of HVC 306-2+230 showing evidence for the interaction between the HVC and the Galactic disk. (a) H I emission at $v = 91 \text{ km s}^{-1}$ and (b) $v = 122 \text{ km s}^{-1}$. The HVC includes all emission over the velocity range $200 - 324 \text{ km s}^{-1}$ and contours are displayed from $2 - 14 \times 10^{19} \text{ cm}^{-2}$ in intervals of $2 \times 10^{19} \text{ cm}^{-2}$. The greyscales are linear with the ranges shown in the wedges at the right of each panel.

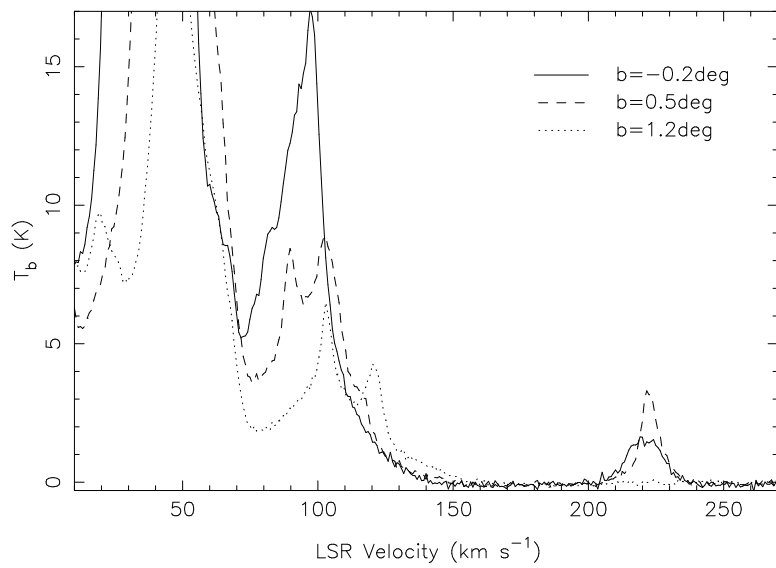


Fig. 2.— H I spectra at $l = 305.8^\circ$ towards $b = -0.2^\circ$ (solid line), $b = 0.5^\circ$ (dashed line), and $b = 1.2^\circ$ (dotted line), through the HVC tail, the HVC head and the ridge off the dense end of the HVC, respectively. All spectra show a peak at $v_{LSR} \sim 100 \text{ km s}^{-1}$, but the spectra towards the cap and the head of the HVC show an additional feature near $v_{LSR} \sim 120 \text{ km s}^{-1}$, which seems to have a spatial correlation with the HVC and which we interpret as arising from Galactic disk gass swept up by the HVC.

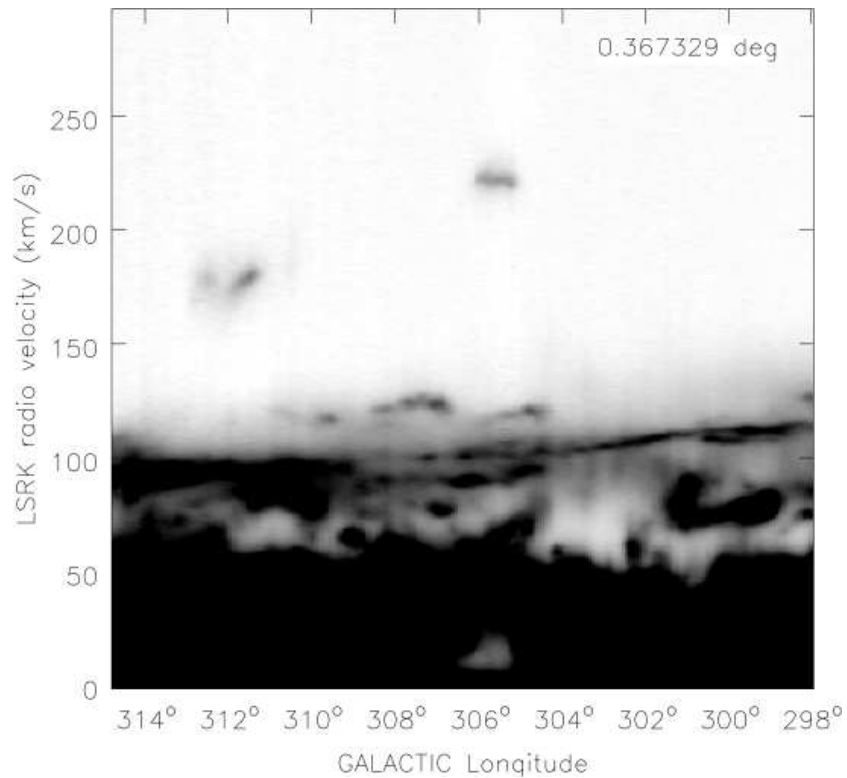


Fig. 3.— Longitude-velocity (l, v) display of the GASS H I data showing the ridge of disk H I at $V_{LSR} \approx 120$ km s^{-1} coincident with HVC 306-2+230. This longitude cut was taken through the head of the HVC at $b = 0.37^\circ$. The ridge is localized between HVC 306-2+230 and another Leading Arm cloud, HVC 312+1+180. The greyscale is linear between -0.2 and 10 K.

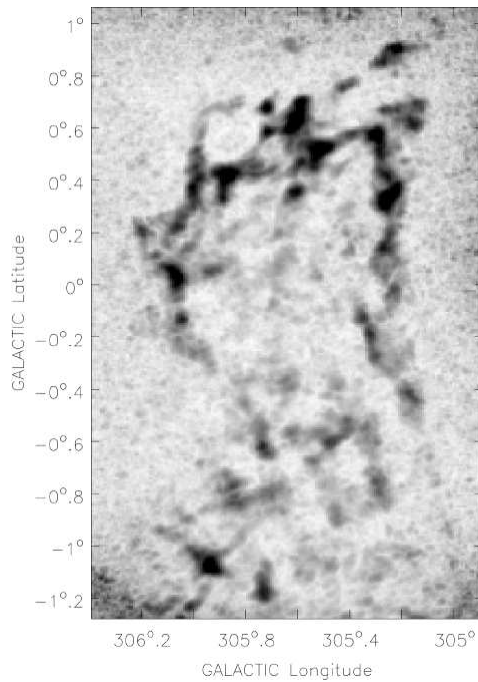


Fig. 4.— High resolution H I image of HVC 306-2+230. The image is of H I peak brightness temperature in the velocity range $175 - 300 \text{ km s}^{-1}$, which covers the HVC only. The greyscale is linear between 2 and 20 K. The image has an angular resolution of $100''$ and a rms brightness temperature noise of $\sim 1.3 \text{ K}$. The cloud shows a very narrow ridge of emission around the head of the cloud, consistent with a bow-shock morphology.

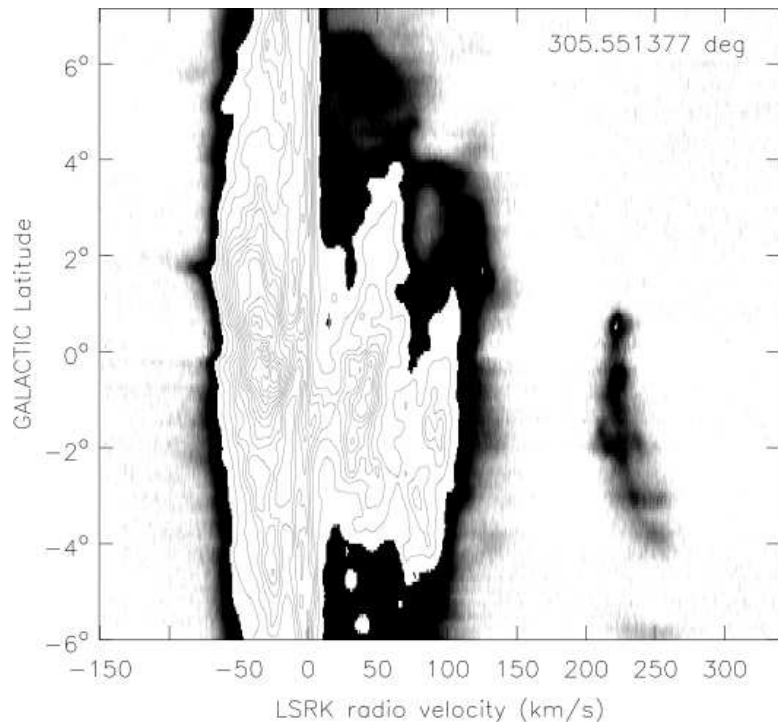


Fig. 5.— Latitude-velocity image of H I emission at $l = 306^\circ$ showing the velocity of HVC 306-2+230 changing from 223 km s^{-1} at $b = -1.5^\circ$ to 252 km s^{-1} at $b = -4.4^\circ$. The greyscale has a power law scaling of -0.5 and goes between $0 - 2 \text{ K}$. H I emission brighter than 5 K is displayed only in contours. We interpret the velocity gradient in the HVC as arising from drag caused by its encounter with the Galactic disk.